Supporting Information for

High Density Ruthenium Single Atoms Anchored on Oxygen Vacancy-Rich g-C_3N_4-C-TiO_2 Heterostructural Nanosphere for Efficient Electrocatalytic Hydrogen Evolution Reaction

Zelin Li, Ying Yang,* Shuangxi Wang, Lin Gu, Shuai Shao

State Key Laboratory of Heavy Oil Processing, China University of Petroleum, Changping, Beijing 102249, China

Email: yyang@cup.edu.cn

Materials and methods

1. Chemicals

Thiourea (CH_4N_2S, 99.0 wt%), ethanol (C_2H_6O, 99.7 wt%), acetone (C_3H_6O, 99.5 wt%), nitric acid (HNO_3, 66.5 wt%), and phosphate buffer saline (PBS, 0.1 M) aqueous solutions were purchased from Beijing Chemical Works. Ruthenium chloride hydrate ($RuCl_3 \cdot xH_2O$, 38.0 wt%), platinum carbon (Pt/C, 20 wt%), ruthenium oxide (RuO_2, 99.9 wt%), and nafion solution were commercially obtained and purchased from Aladdin Chemical Co. Ltd. All the chemicals used in this study are of analytical grade without further purification. Titanium-containing wipe fibers were purchased from Shanghai Meixin Sanitary Products Co. Ltd.

2. Synthesis

2.1. Synthesis of Ru/g-C_3N_4

The synthesis of Ru/g-C_3N_4 was performed by anchoring Ru species on g-C_3N_4. Typically, 10 g of thiourea was heated to 550 ^oC a heating rate of 5 ^oC min^{-1}, and was kept at this temperature for 2 h, affording graphitic carbon nitride, g-C_3N_4. Then 13 mg of g-C_3N_4 was used as the support to anchor Ru species according to the method depicted in Experimental Section 2.1.

2.2. Synthesis of Ru/g-C_3N_4-C

Typically, titanium-containing wipe fiber (TiWF) was first calcinated at 550 ^oC in a N_2 flow for 2 h, yielding carbon-titanium composite, C-TiO_2. The obtained C-TiO_2 was then washed with HF, affording the carbon material, C. The obtained C (0.2 g) combined with 1.5 g thiourea was dispersed in 20 mL of water. The mixture was

transferred into a Teflon-lined stainless steel autoclave and heated at 100 ^{o}C for 24 h. After cooling to room temperature, the solid product was heated to 550 ^{o}C in a N_2 flow at rate of 5 ^{o}C min^{-1}, and was kept at this temperature for 2 h, yielding graphitic carbon nitride-carbon composite, g-C_3N_4-C. Finally, 13 mg of g-C_3N_4-C was used as the support to anchor Ru species according to the method depicted in Experimental Section 2.1.

2.3. Synthesis of Ru/C-TiO_2

The synthesis of Ru/C-TiO_2 was performed by anchoring Ru species on C-TiO_2. Typically, 13 mg of the C-TiO_2 was used as the support to anchor Ru species according to the method depicted in Experimental Section 2.1.

Table S1. EXAFS fitting parameters at the Ru K-edge for various samples.

Sample	Absorber-scatter pair	Coordination number	Bond distance (Å)	σ^2 (10^{-3} Å)[a]	ΔE_0[a] (eV)	R factor
Ru/g-C_3N_4-C-TiO$_2$	Ru-O/N	4.13 ± 0.35	2.039	5.85	2.5	0.0050
Ru/g-C_3N_4	Ru-N	4.14 ± 0.48	2.045	5.76	-9.0	0.0076
$RuCl_3$	Ru-Cl	3	2.423	2.37	9.6	0.0109
Ru foil	Ru-Ru	12	2.672	2.91	3.8	0.0177
RuO_2	Ru-O	6	1.979	2.56	-1.8	0.0142

[a] σ^2 = Debye-Waller factor and ΔE_0 = inner potential correction.

Table S2. Comparison of the HER performance of various electrocatalysts in 1.0 M KOH.

Catalyst	Current density (mA cm^{-2})	Overpotential (mV)	Tafel slope (mV dec^{-1})	Catalyst loading amount (mg cm^{-2})	Reference
Ru/g-C_3N_4-C-TiO_2	10	107	85	0.226	This work
Ru/C	10	186	125	0.343	[1]
Ru doped $Ni(OH)_2$/TM-0.2	10	135	64	-	[2]
$Rh_{50}Ru_{50}$@UiO-66-NH_2	10	177	112	0.343	[1]
BRP-g-C_3N_4-CPE	10	115	79	-	[3]
Co@BNCNTS	10	187	110	-	[4]
CoO_x@CN	10	232	115	0.420	[5]
MoS_2@Mo-S-C_3N_4	10	290	146	-	[6]
MoC@NCS-1000	10	111	57	-	[7]
Ni-Mn-LDH/g-C_3N_4	10	126	50	-	[8]

Table S3. The calculated H_2O dissociation Gibbs free energy ($|\Delta G_{H2O}|$) and the adsorption free energy of H ($|\Delta G_{H^*}|$) for Vo-g-C_3N_4-C-TiO_2, Ru/P-g-C_3N_4-C-TiO_2 and Ru/Vo-g-C_3N_4-C-TiO_2.

	Vo-g-C_3N_4-C-TiO_2	Ru/P-g-C_3N_4-C-TiO_2	Ru/Vo-g-C_3N_4-C-TiO_2
$\|\Delta G_{H2O}\|$	0.19 eV	1.02 eV	0.88 eV
$\|\Delta G_{H^*}\|$	2.03 eV	1.25 eV	0.41 eV

Table S4 Comparison of the HER performance of various electrocatalysts in 0.5 M H_2SO_4.

Catalyst	Current density (mA cm^{-2})	Overpotential (mV)	Tafel slope (mV dec^{-1})	Catalyst loading amount (mg cm^{-2})	Reference
Ru/g-C_3N_4-C-TiO_2	10	112	65	0.226	This work
C_3N_4-Ru-F	10	140	57	0.153	[9]
MoS_2@Mo-S-C_3N_4	10	193	65	-	[6]
C_3N_4-Cu	10	309	76	0.280	[10]
C_3N_4-nanoribbon-G	10	207	54	0.143	[11]
C_3N_4/NG	10	240	51	0.100	[12]
C_3N_4/AgPt	10	150	65	0.352	[13]
CoO_x/mC@MoS_2@g-C_3N_4	10	98	66	-	[14]
GO-Co_2P	20	67	83	1.33	[15]
N-WS_2–H_2	100	197	70	-	[16]

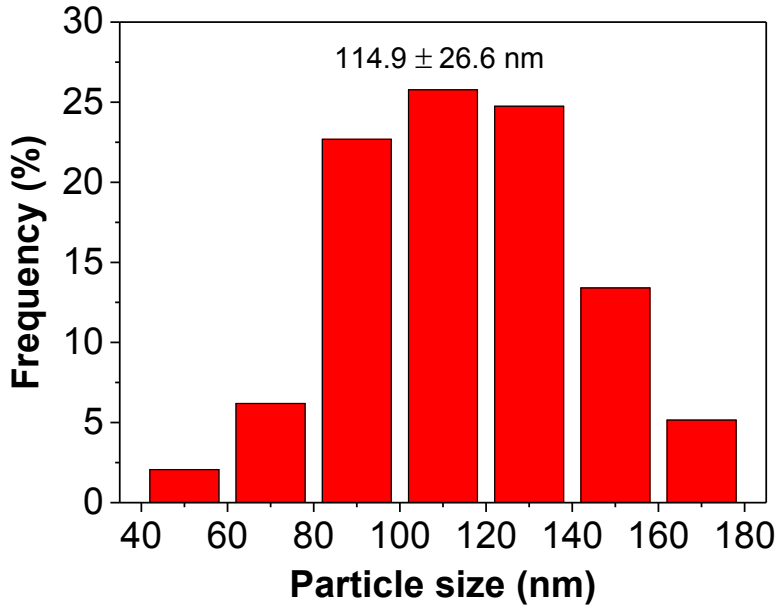

Figure S1. The particle size distribution histogram of g-C_3N_4-C-TiO_2.

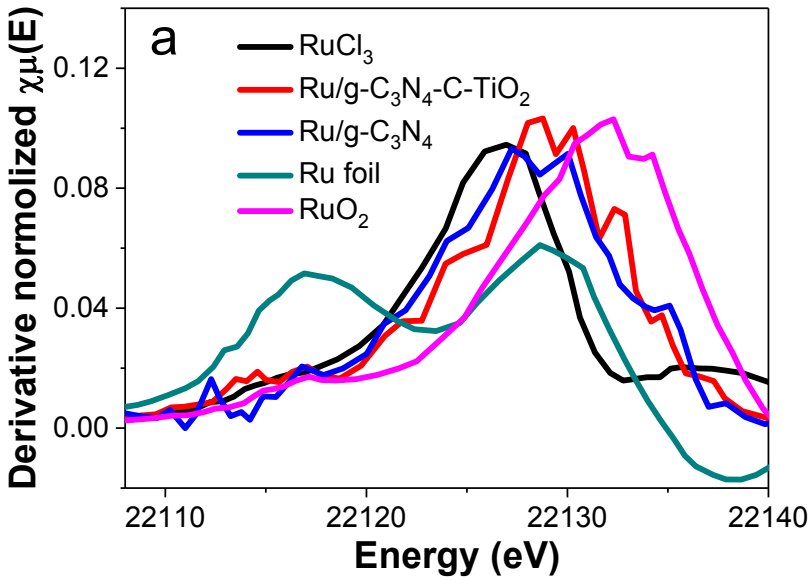

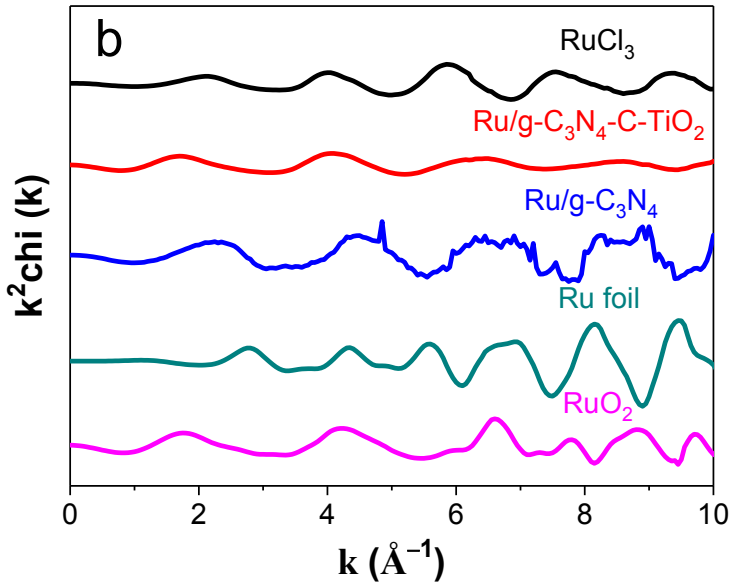
b
RuCl3
Ru/g-C3N4-C-TiO2
Ru/g-C3N4
Ru foil
RuO2
k2chi (k)
0
2
4
6
8
10
k (Å−1)

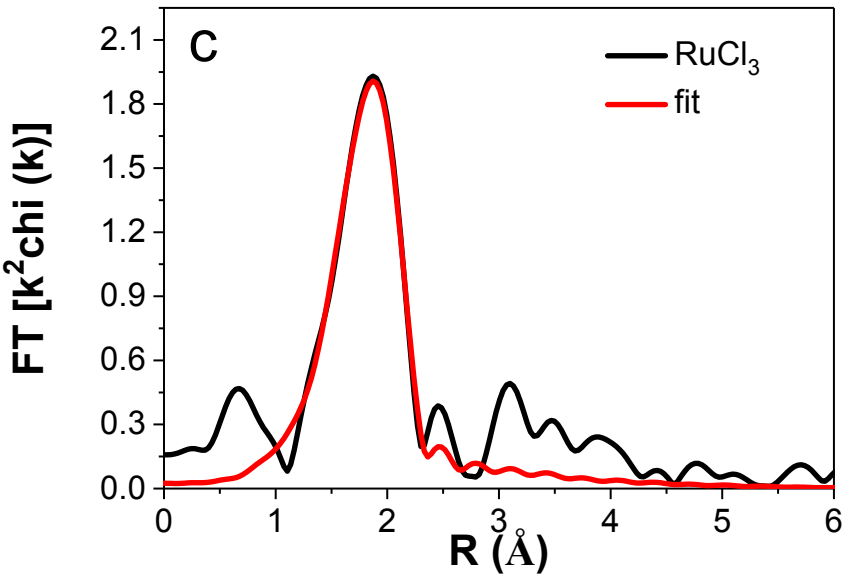
c
RuCl3
fit
FT [k2chi (k)]
2.1
1.8
1.5
1.2
0.9
0.6
0.3
0.0
0
1
2
3
4
5
6
R (Å)

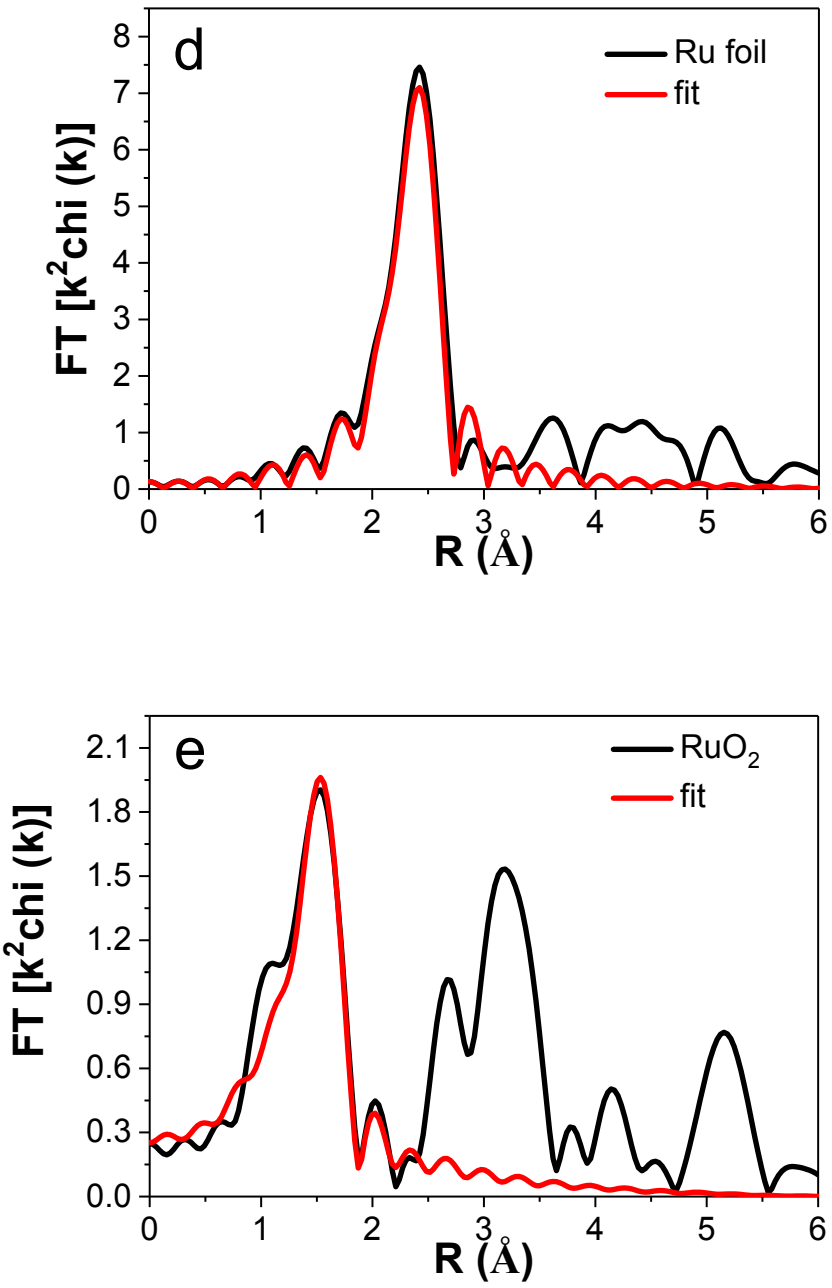

Figure S2. (a) First derivative curves and (b) the k^2-weighted EXAFS spectra at k space for different Ru-containing samples, and EXAFS fitting curve for (c) $RuCl_3$, (d) Ru foil and (e) RuO_2.

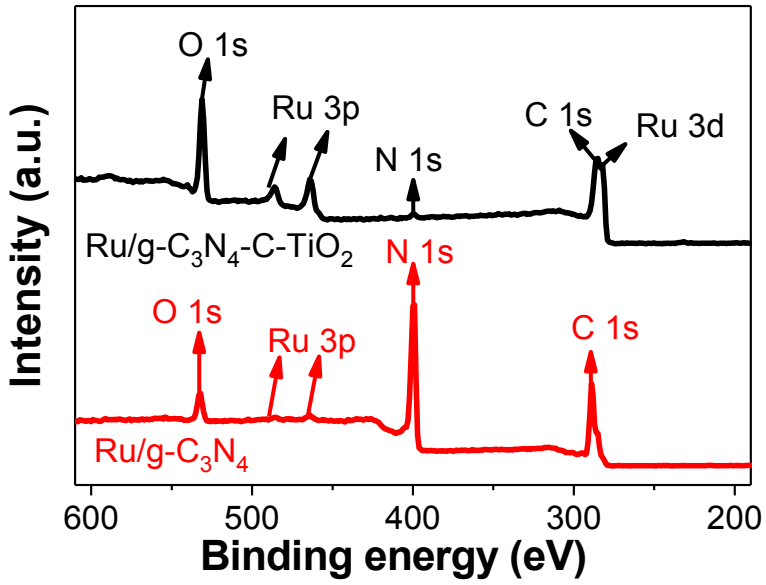

Figure S3. XPS survey spectra of Ru/g-C_3N_4-C-TiO_2 and Ru/g-C_3N_4.

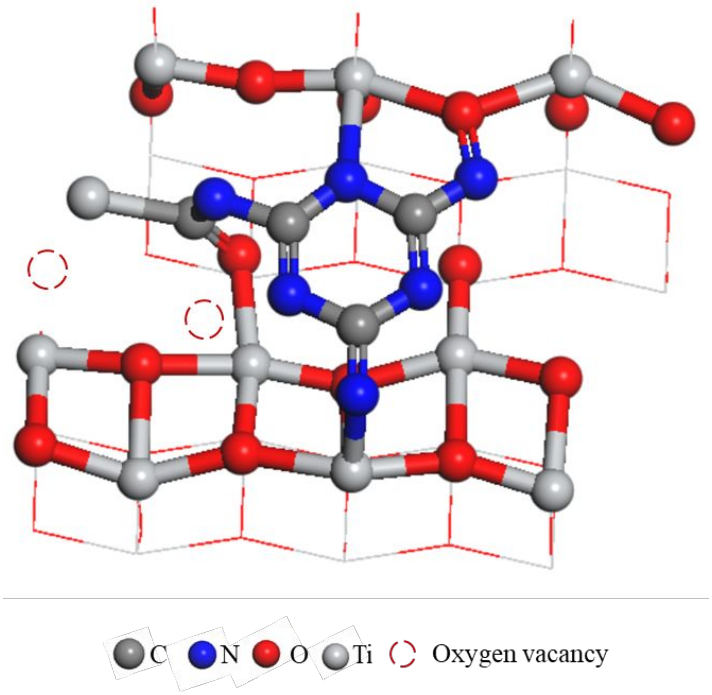

Figure S4. The optimized atomic structure model of Vo-g-C_3N_4-C-TiO_2.

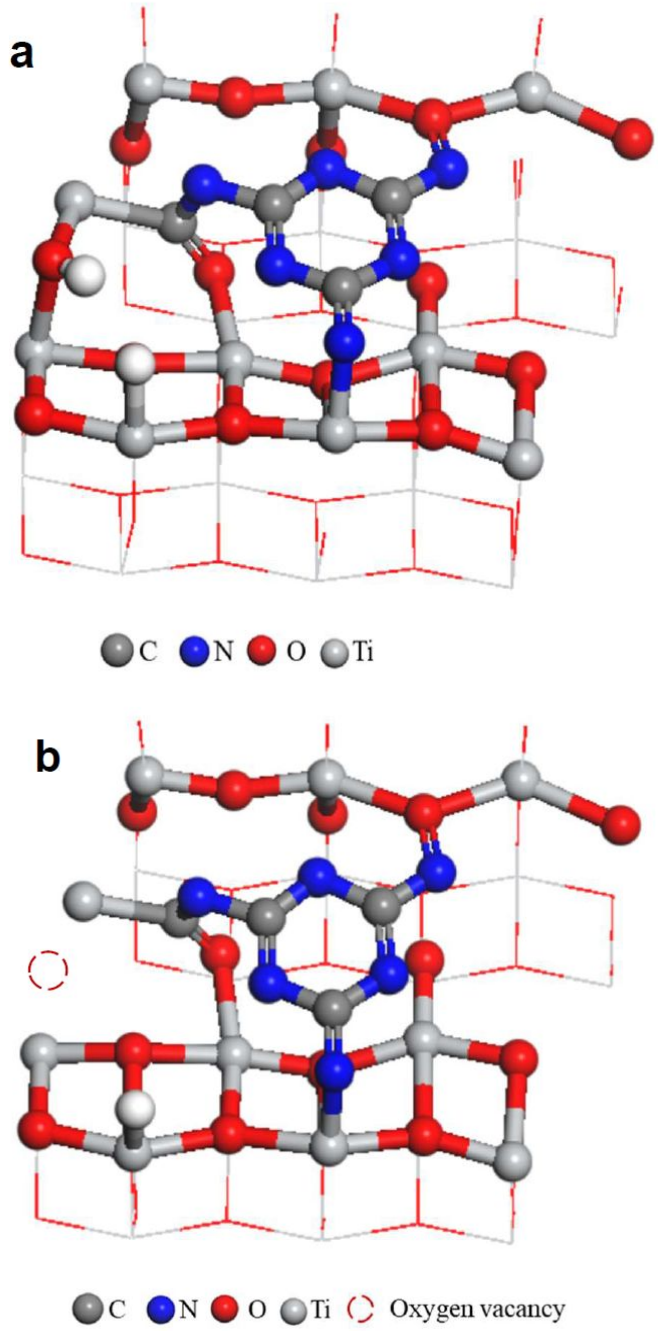

Figure S5. The surface structures of Vo-g-C_3N_4-C-TiO_2 for the reaction pathway for alkaline HER, including (a)ΔG_{H2O} and (b)ΔG_{H*}.

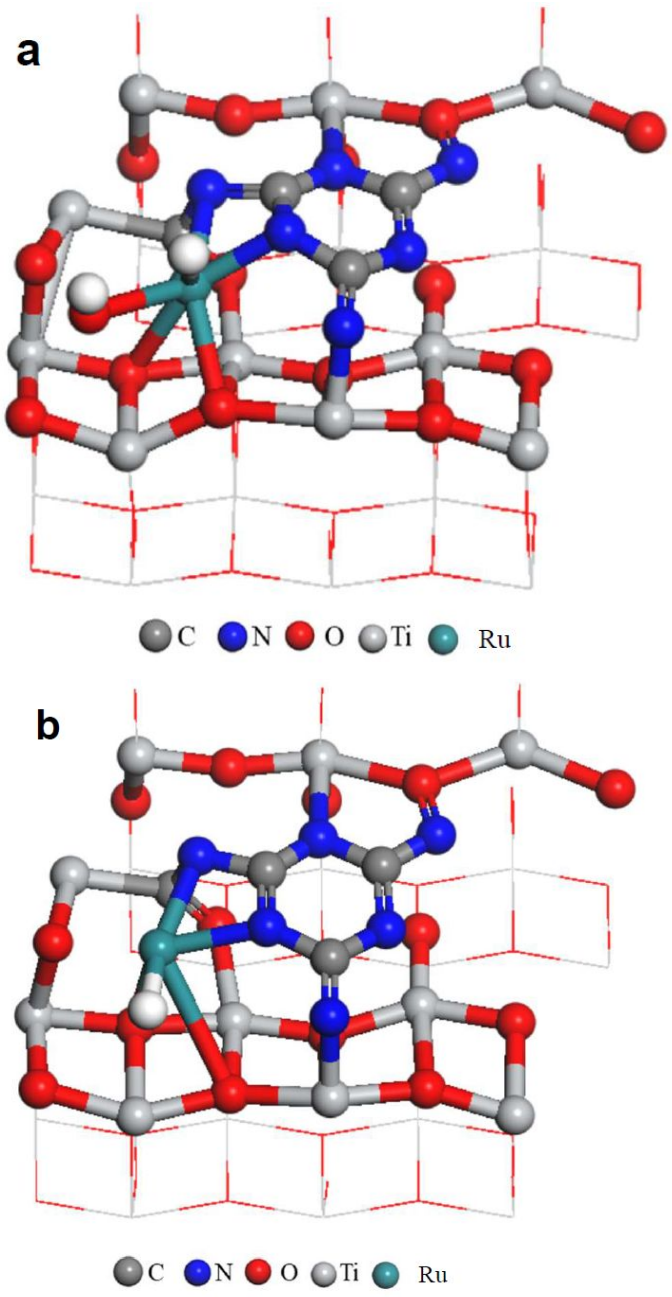

Figure S6. The surface structures of Ru/P-g-C_3N_4-C-TiO_2 for the reaction pathway for alkaline HER, including (a)ΔG_{H2O} and (b)ΔG_{H*}.

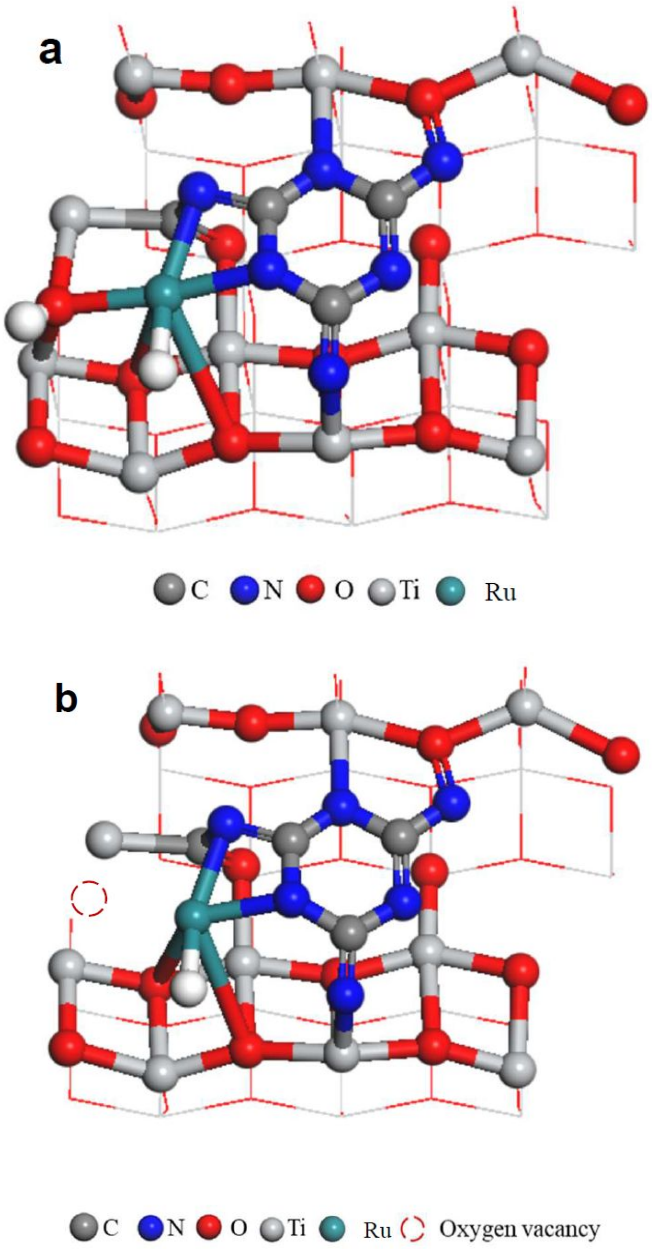

Figure S7. The surface structures of Ru/Vo-g-C_3N_4-C-TiO_2 for the reaction pathway for alkaline HER, including (a)ΔG_{H2O} and (b)ΔG_{H^*}.

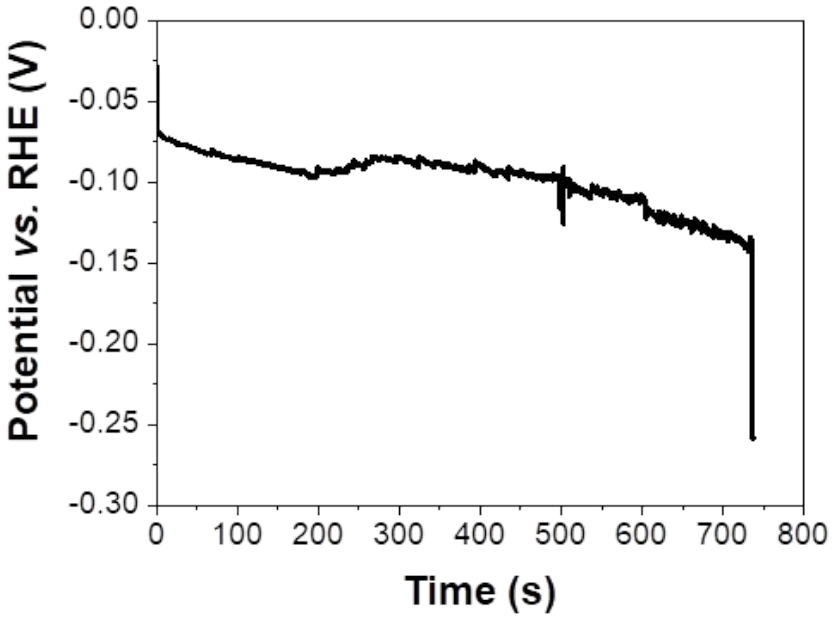

Figure S8. The long-term durability test for Pt/C at constant current density of 10 mA cm^{-2} in 1.0 M KOH.

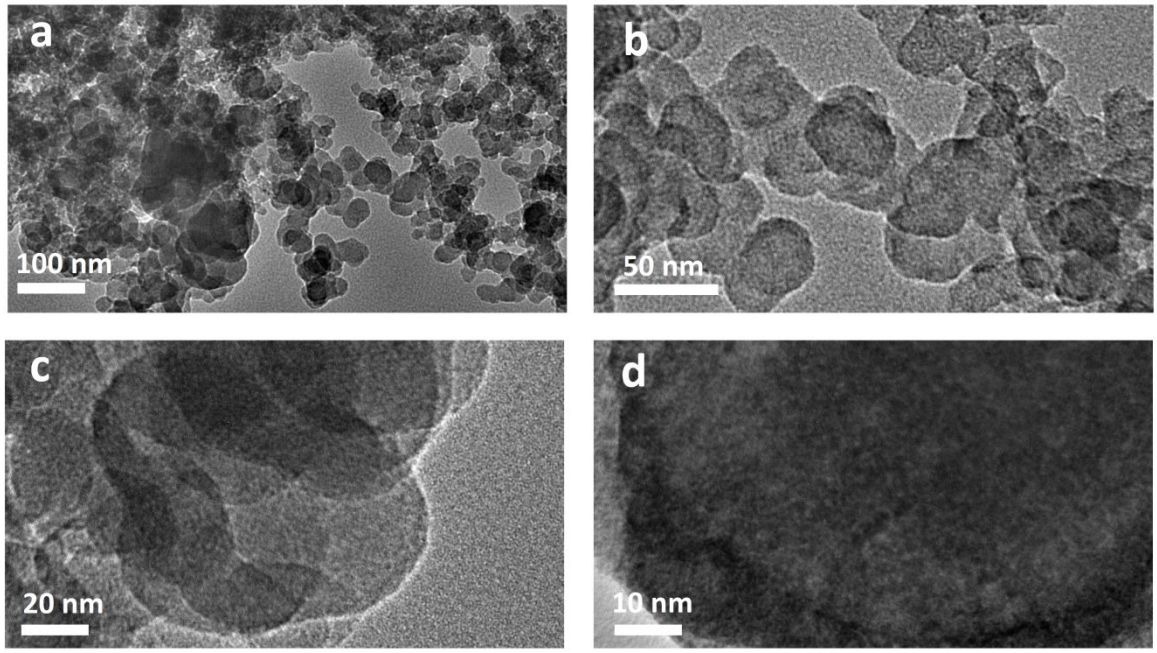

Figure S9. (a,b,c,d) TEM images with a varied magnification for spent Ru/g-C_3N_4-C-TiO_2.

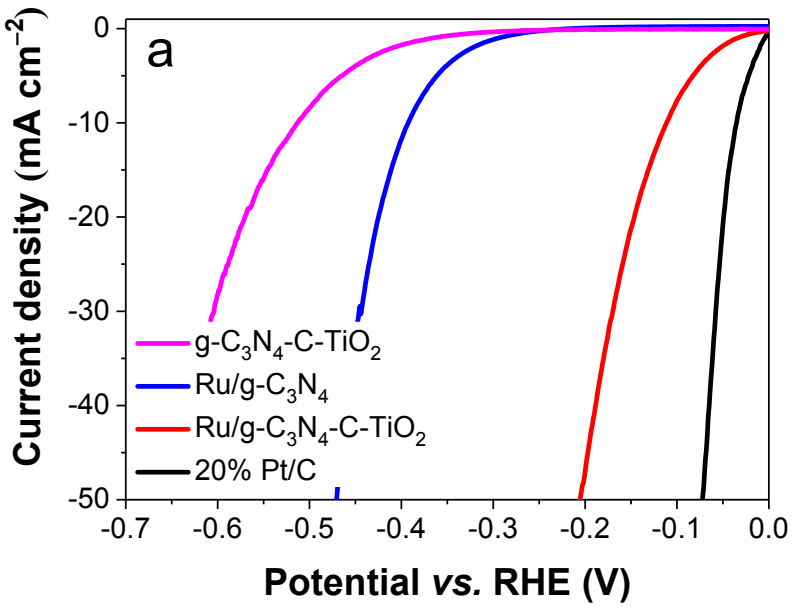
a
Current density (mA cm^{-2})
Potential *vs.* RHE (V)
g-C_3N_4-C-TiO_2
Ru/g-C_3N_4
Ru/g-C_3N_4-C-TiO_2
20% Pt/C
0
-10
-20
-30
-40
-50
-0.7
-0.6
-0.5
-0.4
-0.3
-0.2
-0.1
0.0

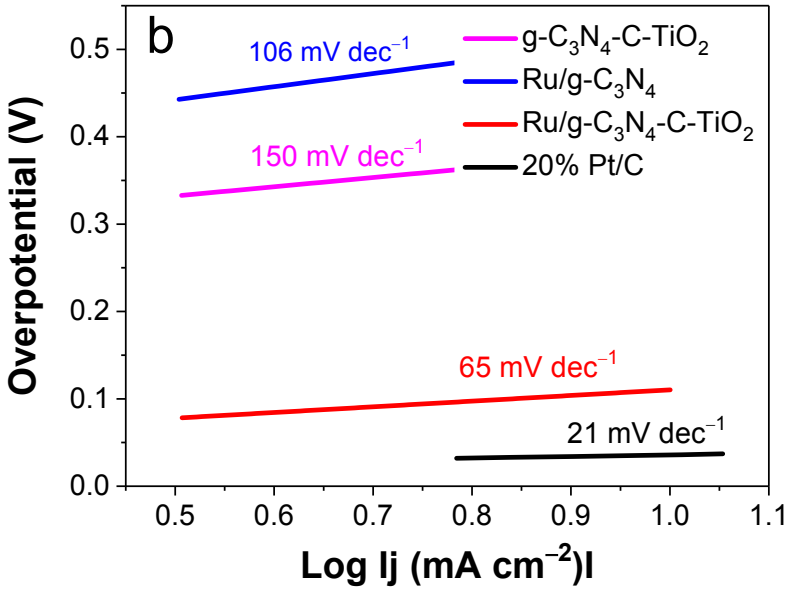
b
Overpotential (V)
Log Ij (mA cm^{-2})I
106 mV dec^{-1}
150 mV dec^{-1}
65 mV dec^{-1}
21 mV dec^{-1}
g-C_3N_4-C-TiO_2
Ru/g-C_3N_4
Ru/g-C_3N_4-C-TiO_2
20% Pt/C
0.5
0.4
0.3
0.2
0.1
0.0
0.5
0.6
0.7
0.8
0.9
1.0
1.1

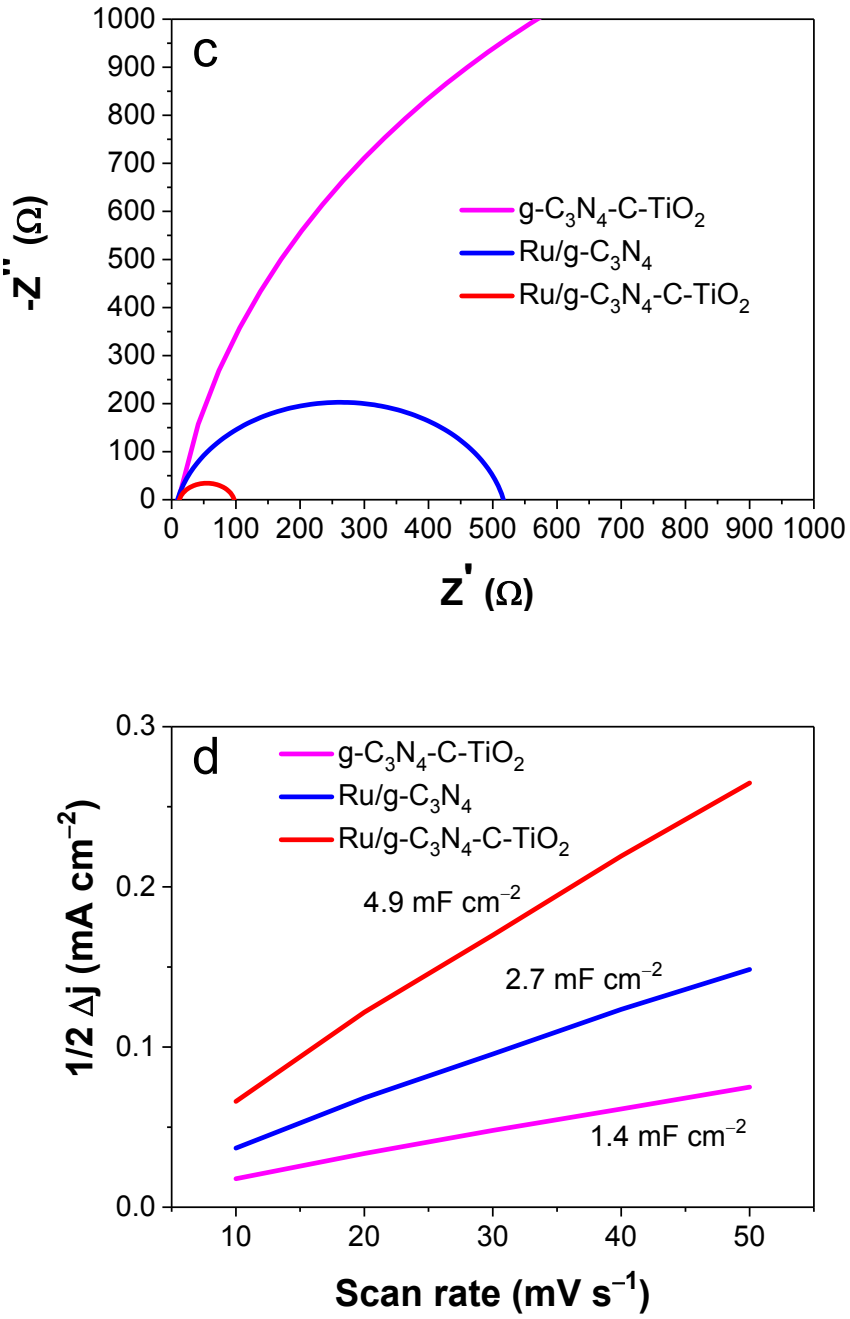

Figure S10. (a) The HER polarization curves of various catalysts in 0.5 M H_2SO_4 and (b) the corresponding Tafel plots, (c) Nyquist plots and (d) C_{dl} for various electrocatalysts.

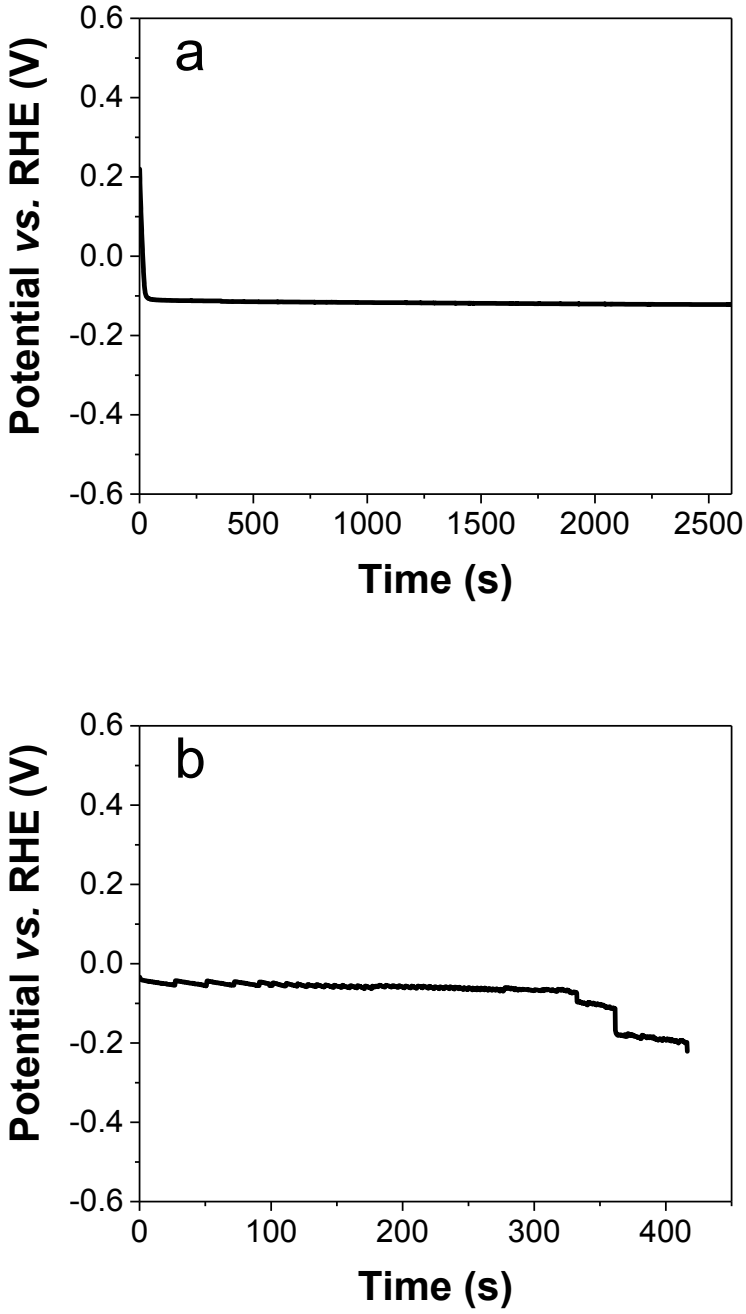

Figure S11. The long-term durability test for (a) Ru/g-C_3N_4-C-TiO_2 and (b)Pt/C at constant current density of 10 mA cm^{-2} in 0.5 M H_2SO_4.

Reference

(1) Wang, Y. J.; Wang, J. K.; Xie, T. P.; Zhu, Q. Y.; Zeng, D.; Li, R.; Zhang, X. D.; Liu, S. L. Ru Doping in $Ni(OH)_2$ to Accelerate Water Reduction Kinetics for Efficient Hydrogen Evolution Reaction. *Appl. Surf. Sci.* **2019**, *485*, 506–512.

(2) Ding, Z. Q.; Wang, K.; Mai, Z. Q.; He, G. Q.; Liu, Z.; Tang, Z. H. RhRu Alloyed Nanoparticles Confined within Metal Organic Frameworks for Electrochemical Hydrogen Evolution at All pH Values. *Int. J. Hydrogen Energy* **2019**, *44* (45), 24680–24689.

(3) Shiravani, F.; Tashkhourian, J.; Haghighi, B. One-step Synthesis of Graphitic Carbon-Nitride Doped with Black-Red Phosphorus as a Novel, Efficient and Free-Metal Bifunctional Catalyst and Its application for Electrochemical Overall Water Splitting. *Sustainable Energy Fuels* **2021**, *5* (12), 3229–3239.

(4) Yu, Z. C; Yao, K. D.; Zhang, S. Q.; Liu, Y.; Sun, Y. Q.; Huang, W. M.; Hu, N. Morphological and Reactive Optimization of g-C_3N_4-Derived Co, N-codoped Carbon Nanotubes for Hydrogen Evolution Reaction Dagger. *New J. Chem.* **2021**, *45* (14), 6308–6314.

(5) Jin, H.; Wang, J.; Su, D.; Wei, Z.; Pang, Z.; Wang, Y. In Situ Cobalt-Cobalt Oxide/N-Doped Carbon Hybrids as Superior Bifunctional Electrocatalysts For Hydrogen and Oxygen Evolution. *J. Am. Chem. Soc.* **2015**, *137* (7), 2688−2694.

(6) Zhang, B. Y.; Li, J. Q.; Song, Q. Q.; Xu, X. T.; Hou, W. F.; Liu, H. Transferable Active Centers of Strongly Coupled MoS_2@Sulfur and Molybdenum Co-doped g-C_3N_4 Heterostructure Electrocatalysts for Boosting Hydrogen Evolution Reaction in

Both Acidic and Alkaline Media. *Inorg. Chem.* **2021**, *60* (4), 2604–2613.

(7) Ren J. T.; Chen L.; Weng C. C.; Yuan G. G.; Yong Z. Well-Defined Mo_2C Nanoparticles Embedded in Porous N-Doped Carbon Matrix for Highly Efficient Electrocatalytic Hydrogen Evolution. *ACS Appl. Mater. Interfaces* **2018**, *10* (39), 33276−33286.

(8) Shakeel, M.; Arif, M.; Yasin, G. Layered by Layered Ni-Mn-LDH/g-C_3N_4 Nanohybrid for Multi-Purpose Photo/Electrocatalysis: Morphology Controlled Strategy for Effective Charge Carriers Separation. *Appl. Catal. B: Environ.* **2019**, *242*, 485−498.

(9) Peng, Y.; Lu, B.; Chen, L.; Wang, N.; Lu, J. E.; Ping, Y.; Chen, S. Hydrogen Evolution Reaction Catalyzed by Ruthenium Ion-Complexed Graphitic Carbon Nitride Nanosheets. *J. Mater. Chem. A* **2017**, *5* (34), 18261−18269.

(10) Zou, X.; Silva, R.; Goswami, A.; Asefa, T. Cu-Doped Carbon Nitride: Bio-Inspired Synthesis of H_2-Evolving Electrocatalysts Using Carbon Nitride (g-C_3N_4) as a Host Material. *Appl. Surf. Sci.* **2015**, *357*, 221−228.

(11) Zhao, Y.; Zhao, F.; Wang, X.; Xu, C.; Zhang, Z.; Shi, G.; Qu, L. Graphitic Carbon Nitride Nanoribbons: Graphene-Assisted Formation and Synergic Function for Highly Efficient Hydrogen Evolution. *Angew. Chem. Int. Ed.* **2014**, *53* (50), 13934−13939.

(12) Zheng, Y.; Jiao, Y.; Zhu, Y.; Li, L. H.; Han, Y.; Chen, Y.; Du, A.; Jaroniec, M.; Qiao, S. Z. Hydrogen Evolution by a Metal-Free Electrocatalyst. *Nat. Commun* **2014**, *5* (4), 3783.

(13) Nazir, R.; Fageria, P.; Basu, M.; Pande, S. Decoration of Carbon Nitride Surface with Bimetallic Nanoparticles (Ag/Pt, Ag/Pd, and Ag/Au) *via* Galvanic Exchange for Hydrogen Evolution Reaction. *J. Phys. Chem. C* **2017**, *121* (36), 19548−19558.

(14) Karuppasamy, K.; Jothi, V. R.; Vikraman, D.; Prasanna, K.; Maiyalagan, T.; Sang, B. I.; Yi, S. C.; Kim, H. S. Metal-Organic Framework Derived NiMo Polyhedron as an Efficient Hydrogen Evolution Reaction Electrocatalyst. *Appl. Surf. Sci.* **2019**, *478*, 916−923.

(15) Sharma, A. K.; Joshi, H.; Ojha, K.; Singh, A. K. Graphene Oxide Supported Cobalt Phosphide Nanorods Designed from a Molecular Complex for Efficient Hydrogen Evolution at Low Overpotential. *Chem. Commun.* **2019**, *55*(15), 2186−2189.

(16) Sun, C. Q.; Zhang, J. Y.; Ma, J.; Liu, P. T.; Gao, D. Q.; Tao, K.; Xue, D. S. N-Doped WS_2 Nanosheets: a High-Performance Electrocatalyst for the Hydrogen Evolution Reaction. *J. Mater. Chem. A* **2016,** *4*(9), 11234–11238